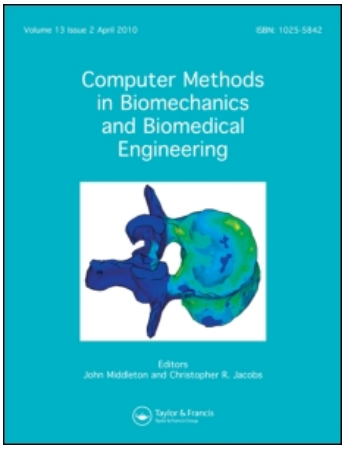

Computer Methods in Biomechanics and Biomedical Engineering
Publication details, including instructions for authors and subscription information:
http://www.informaworld.com/smpp/title~content=t713455284

Modelling of non-linear elastic tissues for surgical simulation

Sarthak Misra[a]; K. T. Ramesh[b]; Allison M. Okamura[b]
[a] University of Twente, Enschede, The Netherlands [b] The Johns Hopkins University, Baltimore, MD, USA

First published on: 25 May 2010

To cite this Article Misra, Sarthak , Ramesh, K. T. and Okamura, Allison M.(2010) 'Modelling of non-linear elastic tissues for surgical simulation', Computer Methods in Biomechanics and Biomedical Engineering,, First published on: 25 May 2010 (iFirst)
To link to this Article: DOI: 10.1080/10255840903505121
URL: http://dx.doi.org/10.1080/10255840903505121

Computer Methods in Biomechanics and Biomedical Engineering
iFirst article, 2010, 1–8

Modelling of non-linear elastic tissues for surgical simulation

Sarthak Misra[a]*, K.T. Ramesh[b] and Allison M. Okamura[b]

[a]*University of Twente, Enschede, The Netherlands;* [b]*The Johns Hopkins University, Baltimore, MD, USA*

(*Received 22 June 2009; final version received 19 November 2009*)

Realistic modelling of the interaction between surgical instruments and human organs has been recognised as a key requirement in the development of high-fidelity surgical simulators. Primarily due to computational considerations, most of the past real-time surgical simulation research has assumed linear elastic behaviour for modelling tissues, even though human soft tissues generally possess non-linear properties. For a non-linear model, the well-known Poynting effect developed during shearing of the tissue results in normal forces not seen in a linear elastic model. Using constitutive equations of non-linear tissue models together with experiments, we show that the Poynting effect results in differences in force magnitude larger than the absolute human perception threshold for force discrimination in some tissues (e.g. myocardial tissues) but not in others (e.g. brain tissue simulants).

Keywords: haptics; hyperelasticity; Poynting effect; non-linear elasticity; soft tissue mechanics; surgical simulation

1. Introduction

Surgical simulation systems are an attractive option for surgical training, practice and both pre- and intra-operative planning. In addition, such simulators help in optimising surgical tool design and understanding tissue injury mechanisms and damage thresholds (De et al. 2007). These systems allow real-time visualisation of a surgical procedure and, in some cases, provide force feedback to the user. The development of realistic simulation systems that provide appropriate haptic feedback requires accurate modelling of soft tissue and their interaction with surgical tools. Human organs, in general, are inhomogeneous and anisotropic and exhibit non-linear viscoelastic properties (Fung 1993). Due to limits in computation speed and memory, simplified models are frequently used to describe tissues for simulating surgical procedures, such as mass-spring-damper or linear elastic models (Gibson and Mirtich 1997). Such models are only accurate for materials undergoing small strains, while most surgical procedures involve organs being subjected to large strains. The theory of non-linear elasticity (hyperelastic models) better describes many human tissues undergoing large strains.

Given the complexity of human organs and challenges in acquisition of tissue parameters, realistic modelling and simulation of tissue deformation is an ongoing research area. Extensive work has been done by researchers in the area of computer graphics to model deformable bodies (Nealen et al. 2006). In such studies, the focus has been to produce seemingly realistic visualisation, while ignoring the physics underlying tissue deformation. On the other hand, there exists a rich literature in the biomechanics community involving the measurement and characterisation of tissue properties of specific organs (e.g. Yamada 1970; Fung 1993).

Within the robotics and haptics research communities, much of the past research has assumed linear elasticity for modelling tissues for both invasive and non-invasive surgical procedures (Misra et al. 2008a). Researchers have also investigated a wide variety of methods for modelling tool–tissue interactions based on techniques other than continuum mechanics (e.g. Delingette et al. 1994; James and Pai 2001; Sundaraj et al. 2002). The primary reason for using such non-physical modelling techniques is computational efficiency. Famaey and Vander Sloten (2008) and Misra et al. (2008a) provide an overview of organ modelling methods (physical and non-physical) applied to surgical simulation. In this paper, we demonstrate that there is a significant difference between the forces applied to the user for linear and non-linear elastic tissue models. While this is not a new concept, our work provides a concrete example of how modelling techniques relate to human perception of surgical simulators. In addition to this paper and its precursors (Misra et al. 2007, 2008b), Dehghan and Salcudean (2006) have compared the effects of linear and non-linear finite element models on mesh displacement during needle insertion. Dehghan and Salcudean (2006) concluded that, in the presence of asymmetric boundary conditions, there are noticeable differences between linear and non-linear models.

In this paper, we examine the role of the Poynting effect in modelling tissue deformation for surgical simulation. The Poynting effect describes the interaction

*Corresponding author. Email: s.misra@utwente.nl

ISSN 1025-5842 print/ISSN 1476-8259 online

DOI: 10.1080/10255840903505121
http://www.informaworld.com

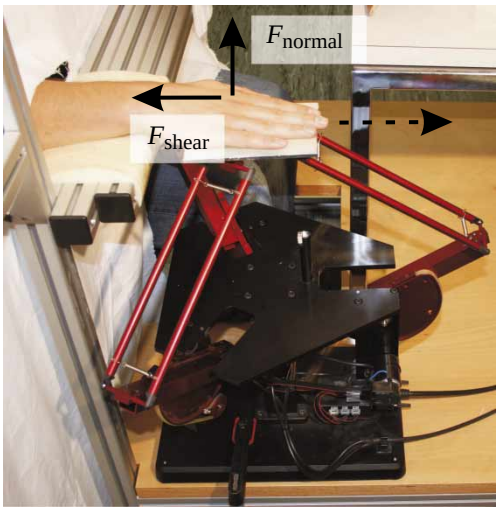

Figure 1. As the user interacts with the non-linear elastic virtual model and moves the Delta haptic device (Force Dimension, Nyon, Switzerland), normal (F_{normal}) and shear (F_{shear}) forces are generated due to the Poynting effect. Psychophysical experiments using this haptic device showed that both shear and normal forces affect user perception (Misra et al. 2009). The Mooney–Rivlin strain energy function with properties of liver was used as the virtual material model. The virtual model produces the interaction forces based on the non-linear constitutive equations.

of both shear (tangential) and normal forces during tissue shearing. Shear is a common mode of organ deformation either during surgical tool–tissue interaction or during palpation by the clinician's hand. Figure 1 provides a visual representation of the forces developed while shearing a non-linear elastic virtual model using a haptic device. We first provide a description of specific non-linear elastic tissue models that highlight the Poynting effect. This is followed by experimental studies that demonstrate the relevance of this effect for some tissues in surgical simulations. Our work provides a quantitative measure of how tissue modelling techniques relate to human perception of surgical simulators.

The experimental parameter identification and analysis of non-linear elastic models were accomplished by considering palpation of bovine myocardial tissue and Sylgard 527 A&B silicone dielectric gel (Dow Corning Corporation, Midland, MI, USA) samples, which are often used as models for the human heart and brain tissue, respectively. In order to highlight the Poynting effect, non-linear constitutive laws were derived based on the Ogden and exponential forms of the strain energy function. The Ogden form was used for Sylgard gel, while the anisotropic behaviour of myocardial tissue was captured using the exponential form of the strain energy function.

The remainder of the paper is organised as follows. The derivations for the constitutive law of a body undergoing shear and the Poynting effect are presented in Section 2. Experimental studies to populate our model and demonstration of the Poynting effect in Sylgard gel and myocardial tissue are described in Section 3. Finally, we conclude by summarising the results of our study and discussing their implications for haptic feedback in surgical simulators.

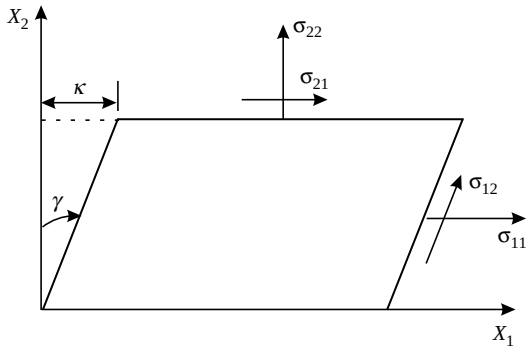

Figure 2. Body undergoing simple shear; the shear strain is κ in the X_1 direction.

2. Coupled normal and shear forces in shearing deformations

We highlight the differences between linear and non-linear elasticity-based tissue models and the role of the Poynting effect in this section. Shearing deformations are considered because it is a common practice for clinicians to palpate and perform a shearing motion on an organ either by hand or by an instrument.

2.1 Non-linear elastic materials

The formulation presented here highlights only the important relationships and does not cover the fundamentals of continuum mechanics. For details, we refer the reader to Gurtin (2003). Figure 2 shows a body undergoing simple shear. The body is assumed to be sheared by an amount κ, and γ is the angle the sheared line makes with its original orientation. The shear strain is given by $\kappa = \tan(\gamma)$. If $\mathbf{y}$ represents the position after deformation of a material particle initially located at $\mathbf{X}$, we can describe the simple shear motion by

$$\mathbf{y} = (X_1 + \kappa X_2)\,\mathbf{e}_1 + X_2\mathbf{e}_2 + X_3\mathbf{e}_3, \tag{1}$$

where $\{\mathbf{e}_1, \mathbf{e}_2, \mathbf{e}_3\}$ are the Cartesian base vectors. The above expression implies that shear displacement is being applied to the body, while preventing displacement in the normal direction. From (1), the matrix of the deformation

gradient tensor, **F**, is computed as

$$\mathbf{F} = \frac{\partial \mathbf{y}}{\partial \mathbf{X}} = \begin{bmatrix} 1 & \kappa & 0 \\ 0 & 1 & 0 \\ 0 & 0 & 1 \end{bmatrix}. \quad (2)$$

The deformation of most biological materials under large strains (>1–2%) can be described by the theory of non-linear elasticity, and hyperelastic models are commonly used. For a hyperelastic material, the Cauchy stress tensor, σ, can be derived from a strain energy density function, *W*. There are various formulations for the strain energy density function depending on the material, e.g. Neo-Hookean, Mooney–Rivlin, St Venant–Kirchhoff, Blatz-Ko, Ogden, polynomial or exponential forms.

Using the kinematic relations for a body undergoing simple shear, we now derive the stresses developed in the body for two different types of strain energy functions (Ogden and exponential forms). These constitutive relations are useful to highlight the differences between linear and non-linear elastic models and are also relevant for the experimental studies described later. It should be noted that the Ogden strain energy functions were originally designed to model rubber-like materials, but they are sufficient for the purposes of this study to highlight the differences between linear and non-linear elastic models.

The Ogden strain energy density function in terms of material parameters, μ and α, is of the form

$$W = \frac{2\mu}{\alpha^2}\left(\lambda_1^\alpha + \lambda_2^\alpha + \lambda_3^\alpha - 3\right). \quad (3)$$

The Cauchy stress tensor for homogenous hyperelastic materials of the Ogden form can be derived as

$$\sigma_{ij} = -p\delta_{ij} + \lambda_i \frac{\partial W}{\partial \lambda_j}, \quad (4)$$

where p is the Lagrange multiplier (essentially a pressure), and λ_i $(i = 1, 2, 3)$ and λ_j $(j = 1, 2, 3)$ are the stretch ratios. Using (3) and (4) together with the plane stress condition ($\sigma_{33} = 0$) yields

$$\sigma_{11} = \frac{2\mu}{\alpha}(\lambda^\alpha - 1), \quad (5)$$

$$\sigma_{21} = \frac{2\mu}{\alpha\kappa}(\lambda^\alpha - \lambda^{-\alpha}), \quad (6)$$

$$\sigma_{22} = \frac{2\mu}{\alpha}(\lambda^{-\alpha} - 1), \quad (7)$$

where $\lambda = (1/2)\left(\kappa + \sqrt{4 + \kappa^2}\right)$.

For anisotropic materials, an exponential strain energy function that accounts for tissue anisotropy is often used. This can be expressed as a function of the Green strain tensor components, E_{ij}, and is typically written as

$$W = \frac{c}{2}(e^Q - 1), \quad (8)$$

where $Q = A_1E_{11}^2 + A_2E_{22}^2 + 2A_3E_{11}E_{22} + A_4E_{12}^2 + 2A_5E_{11}E_{12} + 2A_6E_{22}E_{12}$ and c, A_1, A_2, A_3, A_4, A_5 and A_6 are material parameters. The Cauchy stress tensor in terms of the second Piola–Kirchhoff stress tensor, **S**, is given by

$$\sigma = \frac{1}{J}\mathbf{F}\mathbf{S}\mathbf{F}^{\mathrm{T}}, \quad (9)$$

where $S_{ij} = \partial W/\partial E_{ij}$. For the exponential strain energy function, the stresses developed due to simple shear (using (2), (8) and (9)) are

$$\sigma_{11} = c\kappa\left(\frac{A_5}{2} + \kappa\left(\frac{A_3}{2} + A_4 + \frac{3A_6\kappa}{2} + \frac{A_2\kappa^2}{2}\right)\right)e^\beta, \quad (10)$$

$$\sigma_{21} = c\kappa\left(\frac{A_4}{2} + \kappa\left(A_6 + \frac{A_2\kappa}{2}\right)\right)e^\beta, \quad (11)$$

$$\sigma_{22} = c\kappa\left(\frac{A_6}{2} + \frac{A_2\kappa}{2}\right)e^\beta, \quad (12)$$

where

$$\beta = \kappa^2\left(\frac{A_4}{4} + \kappa\left(\frac{A_6}{2} + \frac{A_2\kappa}{4}\right)\right).$$

As seen in (7) and (12) for the Ogden and exponential strain energy functions, respectively, σ_{22} is non-zero. The presence of normal stress, σ_{22}, and the inequality $\sigma_{11} \neq \sigma_{22}$ is a manifestation of the *Poynting effect* and is a result of the material non-linearity.

2.2 Linear elastic materials

The generalised Hooke's law for isotropic materials that relates the Cauchy stress tensor and the infinitesimal strain tensor is given in component form as

$$\sigma_{ij} = \tilde{\lambda}\varepsilon_{kk}\delta_{ij} + 2G\varepsilon_{ij}, \quad (13)$$

where ε_{ij} is the infinitesimal strain, δ_{ij} the Kronecker delta and $\tilde{\lambda}$ and G the Lamé's constants. For a linear elastic body undergoing simple shear, ε_{12} and ε_{21} are the only non-zero infinitesimal strains. Thus, in contrast to the non-linear elastic case, for a homogenous and isotropic body undergoing simple shear, the stress based on linear elasticity, using (13), is derived as

$$\sigma_{12} = \sigma_{21} = 2G\varepsilon_{21}, \quad (14)$$

and all other components of the stress tensor are zero. For the simple shear case, $\kappa = 2\varepsilon_{21}$, hence (14) could be

rewritten as

$$\sigma_{21} = G\kappa, \tag{15}$$

where G is the shear modulus. The constitutive law given in (13) presents a computationally simple and easy to implement formulation, but such models do not allow the Poynting effect.

3. Role of the Poynting effect in soft tissues

We now consider the experimental evidence of the Poynting effect during palpation of Sylgard gel and myocardial tissue using both experiments and simulations. Tissue models solely based on one set of experiments, e.g. compression or indentation tests, are not sufficient to describe tissue deformation characteristics accurately. Combinations of tension/compression and shear/torsion or biaxial tests are essential for accurate tissue characterisation and identification of material properties.

3.1 *Experiments to measure gel/tissue properties*

We performed uniaxial compression and shear experiments on Sylgard gel. These tests were done using the Rheometrics Solids Analyzer (RSA) II (TA Instruments, New Castle, DE, USA). Sylgard gel is commonly used to simulate human brain tissue.

We prepared and tested 20 Sylgard gel samples of dimensions 10 mm × 10 mm and thickness of 1 mm. The indenter had a surface area larger than the dimensions of the tested sample (10 mm × 10 mm). Further, all samples were preconditioned so that reliable stress and strain data were acquired. The stress versus strain plots for the compression and shear studies for five representative cases are given in Figure 3(a) and (b), respectively. In order to obtain the material properties corresponding to the Ogden strain energy density function in (3), we derived the constitutive law for uniaxial compression and shear. The constitutive relations based on the Ogden strain energy density function were fit to the experimental data for Sylgard gel. The stress versus strain relation for a body undergoing simple shear for the Ogden strain energy function is given in (6). Using (4), in terms of the material parameters and the stretch ratio, λ_2 (X_2 being the direction of compression), we derived the compressive stress to be

$$\sigma_{22} = \frac{2\mu\lambda_2^{-\alpha/2}}{\alpha}\left(\lambda_2^{3\alpha/2} - 1\right). \tag{16}$$

The above relation is derived using the fact that for a body under uniaxial compression, $\lambda_1 = \lambda_3 = 1/\sqrt{\lambda_2}$. Also, the strain, ε, in terms of the stretch ratio is

$$\varepsilon = 1 - \lambda_2. \tag{17}$$

Using (6) and (16), the mean Ogden material parameters, μ and α, for the five representative test cases are 836.25 kPa and -0.15, respectively. These material properties were evaluated by simultaneously fitting the experimental data to both the shear and uniaxial compression constitutive relations using the non-linear least-squares algorithm (Levenberg–Marquardt) as implemented in MATLAB® (The MathWorks, Inc., Natick, MA, USA).

The material properties for myocardial tissues were determined by Sacks (2000). Five bovine pericardium tissues of good structural consistency of size 25 mm × 25 mm were tested on the biaxial testing device. The test samples were cut such that the myocardial tissue fibres were aligned at 45° with respect to the biaxial device's testing axes. A detailed description of the testing device and the experimental protocol are presented by Sacks (2000). The material properties for myocardial tissue based on biaxial tests and using the exponential strain energy function given in (10) were computed to be 2.640 kPa, 0.977, 11.201, 7.540, -12.191, -22.406 and

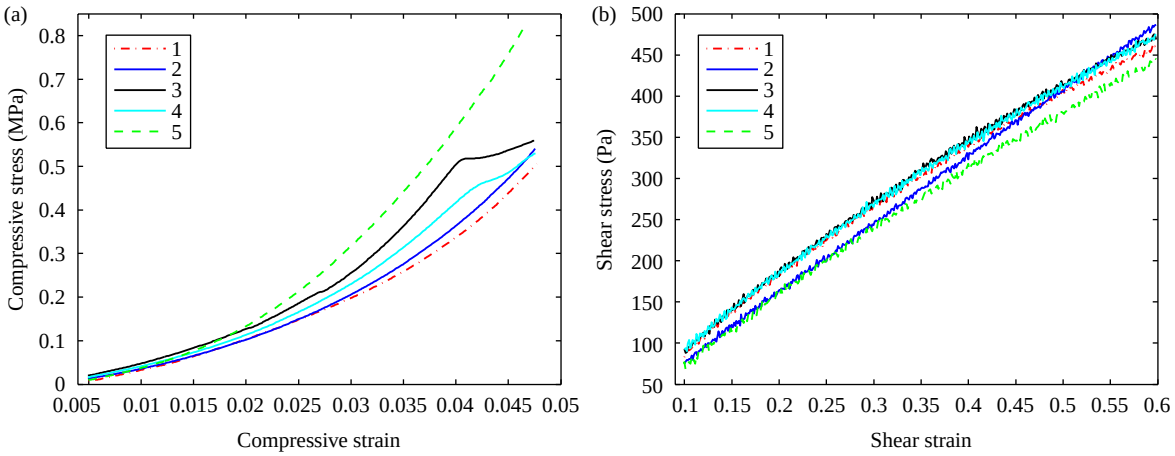

Figure 3. RSA II stress versus strain data for Sylgard gel samples: (a) uniaxial compression and (b) shear.

-4.978 for material parameters c, A_1, A_2, A_3, A_4, A_5 and A_6, respectively (Sacks 2000; Figure 4).

This section presented the material properties for both Sylgard gel and myocardial tissue. These material parameters are used in the analytical models described in Section 2 in order to obtain the stress state of a body undergoing simple shear.

3.2 Observing the Poynting effect

In addition to the acquisition of material parameters of Sylgard gel (using RSA II), large gel samples that are representative of actual organ sizes with dimensions of 100 mm × 50 mm and thicknesses of 5 mm, 7.5 mm and 10 mm were sheared (30%, 50% and 80%) using a robot (Figure 5). The experimental setup was designed to replicate palpation of Sylgard gel. The normal force versus displacement plots generated during shear of two samples are shown in Figure 6. Also, using the Ogden material parameters and analytical expressions for stresses developed during simple shear given in (6) and (7), forces were calculated during shear of samples of dimensions similar to the experiments. The red line in Figure 6 corresponds to the analytically calculated force value. As observed, the normal forces were 0.09 N and 0.07 N for the 5 mm (80% shear) and 10 mm (30% shear) samples, respectively. Figure 7(a) shows both the shear and normal forces developed on the Sylgard gel sample of thickness 10 mm (30% shear). The absolute human perception threshold for force discrimination determined from psychophysical experiments is approximately 0.3 N (Jones 1998). In all our experimental cases, the normal forces generated during palpation of Sylgard gel were less than 0.3 N.

The shear and normal forces predicted to be generated during palpation of myocardial tissue are given in Figure 7(b). These forces were generated using the material properties derived from biaxial tests presented by Sacks (2000) and analytical expressions derived for the simple shear task given in (11) and (12). As has been seen, a normal force of 2.46 N would be generated by a 10% shear of bovine myocardial tissue, which is significantly larger than the absolute human perception threshold for force discrimination. In contrast, the only stress developed for the commonly implemented linear elastic tissue model is $\sigma_{21} = G\kappa$, and all normal forces are masked by the linear elasticity assumption. Thus, depending on the type of tissue (e.g. myocardial tissue versus Sylgard gel) being sheared, the normal forces generated could significantly affect the tissue deformation, as well as the magnitude of force feedback provided during surgical simulation. It should be noted that the coupling between the shear and normal forces in this case is a function of both material anisotropy and material non-linearity, although for large strains, material non-linearity dominates. Figure 7(b) shows that the relationship between the shear and normal forces varies as the shear strain increases for myocardial tissue.

The analysis and experimental results imply that, with a non-linear elastic tissue model in a surgical simulator, the user might perceive noticeably different haptic feedback while interacting with the organ model. A caveat to this statement is that the palpation of only some soft tissues results in significantly large normal forces due to the Poynting effect. Hence, this work emphasises careful examination of relevant simulator design parameters (e.g. soft tissue constitutive laws) that relate to final simulator behaviours.

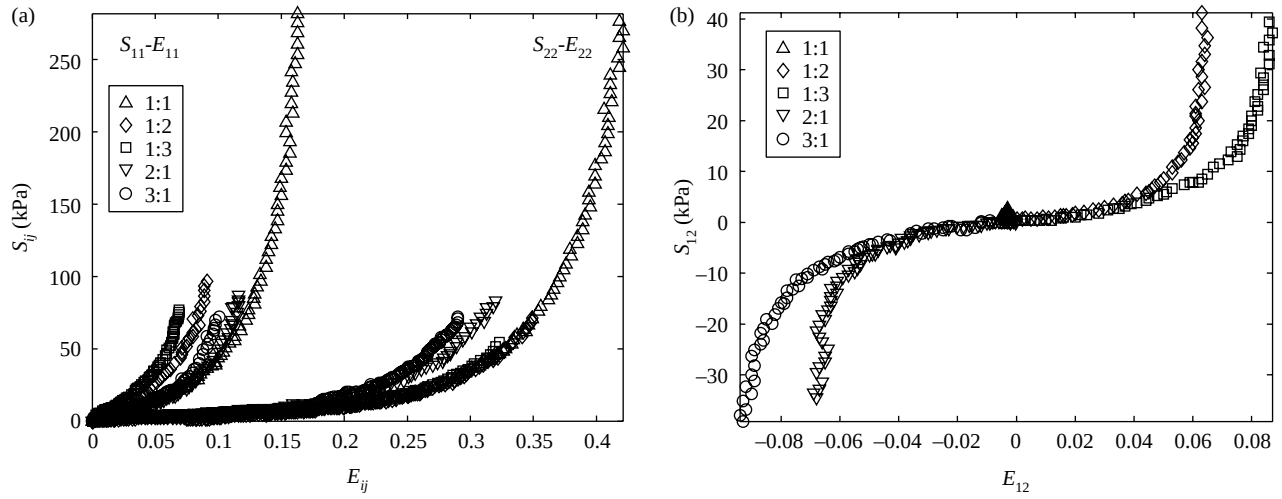

Figure 4. Biaxial test data for myocardial tissue for (a) normal and (b) in-plane shear. The ratios correspond to the applied biaxial stretch E_{11}:E_{22}. These data were digitised from results published by Sacks (2000).

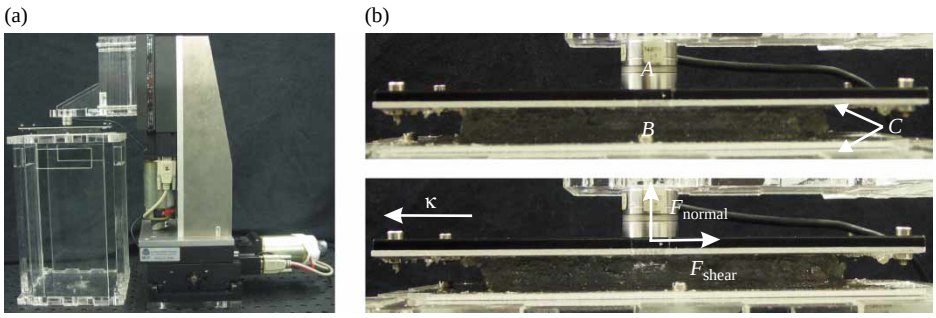

Figure 5. Experimental setup used to perform shear tests on large Sylgard gel samples. (a) Robot with gel and (b) robot shearing the Sylgard gel samples, where *A*, *B* and *C* are the Nano 17 force sensor (ATI Industrial Automation, Apex, NC, USA), gel sample and metal plates used for shearing, respectively. Top: unsheared sample. Bottom: sheared sample.

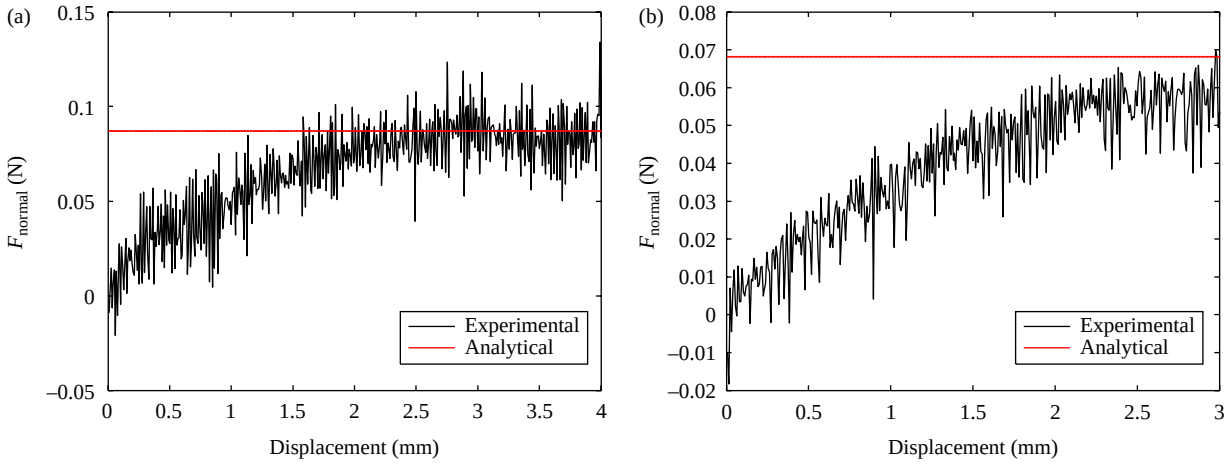

Figure 6. Normal forces generated during the shear of large Sylgard gel samples, (a) 5 mm thick sample sheared at 80% strain and (b) 10 mm thick sample sheared at 30% strain.

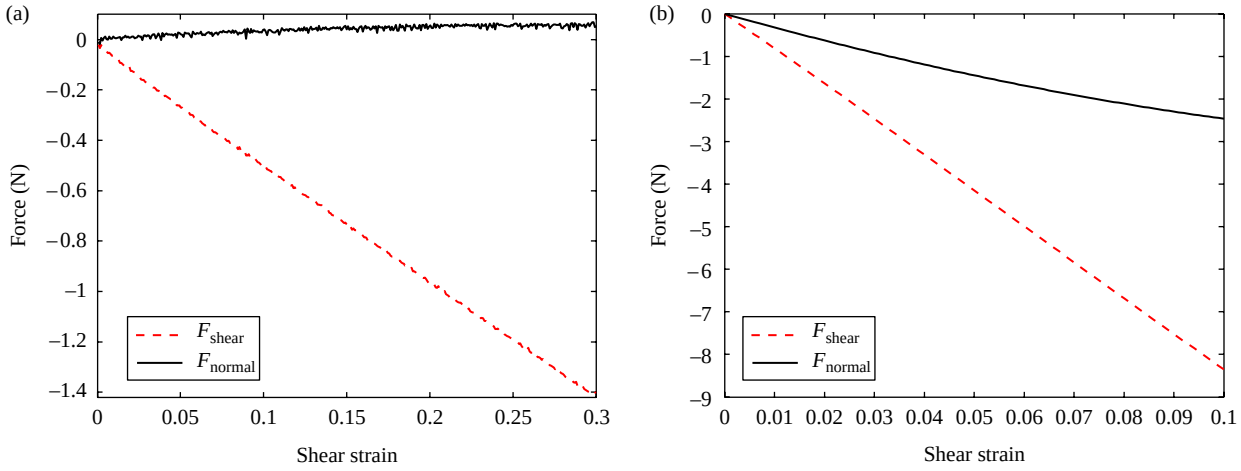

Figure 7. (a) Shear and normal forces developed during palpation (30% shear) of the Sylgard gel sample of dimensions 100 mm × 50 mm × 10 mm (thick). (b) Analytically derived shear and normal forces developed on the shear plane of area 100 mm × 50 mm, during palpation (10% shear) of bovine myocardial tissue. The normal forces developed are due to the Poynting effect and can either be in the positive or negative directions depending on the constitutive equations.

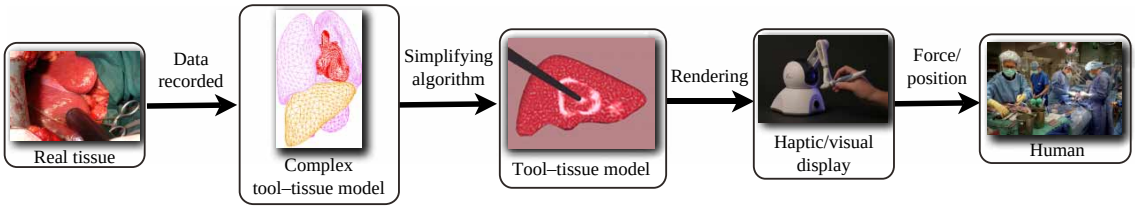

Figure 8. Modelling the information flow in simulator development and application. Each stage acts as a 'filter' in which information about force–motion relationships are lost or transformed. Images are obtained from Eidgenössische Technische Hochschule Zürich (http://www.zfm.ethz.ch/e/biomechanics/), Roberts et al. (2007), Institut National de Recherche en Informatique et en Automatique (http://www.inrialpes.fr/sed/PRV/), SensAble Technologies, Inc. (http://www.sensable.com/haptic-phantom-omni.htm) and Sacred Heart Medical Center (http://www.peacehealth.org/OHVI/CardiacSurgery.htm). Image corresponding to Roberts et al. (2007) is printed with permission from ©2007 Elsevier Ltd.

4. Discussion

The presence of normal forces during shearing of tissue is a consequence of the non-linearity of the material, which is not observed in linear elastic or typical non-physical models. Though linear elastic models are computationally simple and easy to implement, such models do not exhibit the coupling of normal and shear tractions that may be expected from tissues. Depending on the type of tissue (e.g. myocardial tissue and Sylgard gel) being palpated, the normal forces generated could be significant. We showed significant Poynting effect for myocardial tissue but not for Sylgard gel, based on the absolute human perception threshold for force discrimination published in the psychophysics literature. Further, Misra et al. (2009) performed psychophysical experiments to quantify the role of the Poynting effect on material discrimination. Research participants interacted with virtual non-linear elastic tissue models via a haptic device (Figure 1). For non-linear elastic tissue models exhibiting the Poynting effect, our analysis indicated that both shear and normal forces affect user perception.

A fundamental, yet unanswered, research question is what the fidelity of a surgical simulator should be so that realistic haptic feedback is provided to the user. Some researchers evaluate simulator effectiveness using 'expert' surgeon subjective evaluation, while others test the ability of trainees to perform real (usually animal) surgeries before and after using the simulator. We propose another approach, in which we model the flow of information from the real tissue to acquired data, the model, the rendering technique, the haptic and/or visual display and eventually the human user (Figure 8). We conjecture that each of these stages acts as a 'filter' in which information about force–motion relationships are lost or transformed. For example, the filter may be a result of the resolution of the measurement device used for gathering experimental data, the simulation model based on the constitutive law derived from experimental data or simplification of the model required to perform real-time haptic rendering. In addition, haptic devices have their own dynamics and are affected by control issues such as sample-and-hold and quantisation. Finally, human perception plays a vital role in quantifying the necessary fidelity of the simulation.

This study provides a concrete example of how tissue modelling techniques relate to haptic feedback in surgical simulators. Rendering of haptic and/or visual feedback in real time, in conjunction with non-linear tissue models, is possible but computationally intensive, as demonstrated by Székely et al. (2000). The long-term goal of this research is to quantify and understand how organ model fidelity affects realism in surgical simulators and planners. Considering physical phenomena such as the Poynting effect, which is significant for some organs but may not be for others, will allow researchers to make justified simplifications to enable realistic, real-time simulation of tool–tissue interactions.

Acknowledgements

This research was supported by NSF Grant No. EIA-0312551, NIH Grant No. R01-EB002004 and a Link Foundation Fellowship. The authors would like to thank Dr Jack C. Roberts, Dr Andrew M. Lennon and Andrew C. Merkle from the Applied Physics Laboratory, Johns Hopkins University for providing us with the Sylgard gel samples. The authors would also like to acknowledge the help from Matthew Moses (Johns Hopkins University) in conducting the experiments using Sylgard gel.

References

De S, Rosen J, Dagan A, Hannaford B, Swanson P, Sinanan M. 2007. Assessment of tissue damage due to mechanical stresses. Int J Robot Res. 26(11–12):1159–1171.

Dehghan E, Salcudean SE. 2006. Comparison of linear and non-linear models in 2D needle insertion simulation. In: 9th International Conference on Medical Image Computing and Computer Assisted Intervention. Workshop Proceedings on Computational Biomechanics for Medicine; October; Copenhagen, Denmark. p. 117–124.

Delingette H, Subsol G, Cotin S, Pignon J. 1994. A craniofacial surgery simulation testbed. In: Proceedings of the International Conference on Visualization in Biomedical Computing; October; Rochester, NY, USA. p. 607–618.

Famaey N, Vander Sloten J. 2008. Soft tissue modelling for applications in virtual surgery and surgical robotics. Comput Methods Biomech Biomed Eng. 11(4):351–366.

Fung YC. 1993. Biomechanics: mechanical properties of living tissues. 2nd ed. New York (NY): Springer-Verlag.

Gibson SF, Mirtich B. 1997. A survey of deformable modeling in computer graphics. Mitsubishi Electric Research Laboratories, Mitsubishi Electric Corporation. Cambridge, UK. Technical report TR–97–19.

Gurtin ME. 2003. An introduction to continuum mechanics. 1st ed. London: Academic Press.

James D, Pai DK. 2001. A unified treatment of elastostatic contact simulation for real time haptics. Haptics-e, Elect J Haptics Res. 2(1):1–13.

Jones LA. 1998. Perception and control of finger forces. In: Proceedings of the ASME Dynamic Systems and Control Division; November; Anaheim, CA, USA. p. 133–137.

Misra S, Fuernstahl P, Ramesh KT, Okamura AM, Harders M. 2009. Quantifying perception of nonlinear elastic tissue models using multidimensional scaling. In: Proceedings of the 3rd Joint Eurohaptics Conference and Symposium on Haptic Interfaces for Virtual Environment and Teleoperator Systems (World Haptics); March; Salt Lake City, UT, USA. p. 570–575.

Misra S, Okamura AM, Ramesh KT. 2007. Force feedback is noticeably different for linear versus nonlinear elastic tissue models. In: Proceedings of the 2nd Joint Eurohaptics Conference and Symposium on Haptic Interfaces for Virtual Environment and Teleoperator Systems (World Haptics); March; Tsukuba, Japan. p. 519–524.

Misra S, Ramesh KT, Okamura AM. 2008a. Modeling of tool–tissue interactions for computer-based surgical simulation: a literature review. Presence: Teleoperators Vir Environ. 17(5):463–491.

Misra S, Ramesh KT, Okamura AM. 2008b. Physically valid surgical simulators: linear versus nonlinear tissue models. In: Proceedings of the Medicine Meets Virtual Reality; January; Long Beach, CA, USA Studies in Health Technology and Informatics. Amsterdam: IOS Press. p. 293–295.

Nealen A, Müller M, Keiser R, Boxerman E, Carlson M. 2006. Physically based deformable models in computer graphics. Comput Graph Forum. 25(4):809–836.

Roberts JC, Merkle AC, Biermann PJ, Ward EE, Carkhuff BG, Cain RP, O'Connor JV. 2007. Computational and experimental models of the human torso for non-penetrating ballistic impact. J Biomech. 40(1):125–136.

Sacks MS. 2000. Biaxial mechanical evaluation of planar biological materials. J Elasticity. 61(1–3):199–246.

Sundaraj K, Mendoza C, Laugier C. 2002. A fast method to simulate virtual deformable objects with force feedback. In: 7th International Conference on Automation, Robotics, Control, and Vision; December; Singapore. p. 413–418.

Székely G, Brechbühler C, Dual J, Enzler R, Hug J, Hutter R, Ironmonger N, Kauer M, Meier V, Niederer P, et al. 2000. Virtual reality-based simulation of endoscopic surgery. Presence: Teleoperators Vir Environ. 9(3):310–333.

Yamada H. 1970. Strength of biological materials. 1st ed. Baltimore (MD): The Williams & Wilkins Co.